AIP Applied Physics Letters

A low-loss, robust setup for double optical gating of high harmonic generation

Steve Gilbertson, Hiroki Mashiko, Chengquan Li, Sabih D. Khan, Mahendra M. Shakya et al.

Citation: Appl. Phys. Lett. **92**, 071109 (2008); doi: 10.1063/1.2883979

View online: http://dx.doi.org/10.1063/1.2883979

View Table of Contents: http://apl.aip.org/resource/1/APPLAB/v92/i7

Published by the American Institute of Physics.

A low-loss, robust setup for double optical gating of high harmonic generation

Steve Gilbertson, Hiroki Mashiko, Chengquan Li, Sabih D. Khan, Mahendra M. Shakya, Eric Moon, and Zenghu Chang[a)]
J. R. Macdonald Laboratory, Department of Physics, Kansas State University, Manhattan, Kansas 66506, USA

(Received 20 November 2007; accepted 30 January 2008; published online 20 February 2008)

Previously, a second harmonic field was added to a polarization gating field by a Mach–Zehnder interferometer to gate the high harmonic generation process in argon gas. To reduce the losses of the interferometer, we developed a collinear setup consisting of only two quartz plates and a barium borate crystal. The high intensity at the focus allowed the double optical gating to be performed on neon gas. As a result, a supercontinuous spectrum was produced capable of supporting 130 as. There is no delay jitter between the second harmonic field and the polarization gating field associated in this setup, which is necessary for generating stable single isolated attosecond pulses. © *2008 American Institute of Physics*. [DOI: 10.1063/1.2883979]

The shortest single isolated optical pulses, 130 as, were generated by polarization gating (PG) of high harmonic generation.[1–3] The pump pulses were generated by combining two counter-rotating circularly polarized laser pulses with a proper delay.[4,5] The duration of each circularly polarized pulse was 5 fs.[1] By adding a weak second harmonic (SH) field to the PG pulses, it is expected that single, isolated attosecond pulses can be generated by using multicycle laser pulses (as long as 12 fs) that are much easier to reproduce daily than the two cycle ones.[6] Since this technique combined the PG with the two-color gating, it is named double optical gating (DOG).

DOG was previously demonstrated with a Mach–Zehnder interferometer.[6] The linearly polarized laser pulses from a hollow-core fiber and chirped mirror compressor[7,8] were frequency doubled with a barium borate (BBO) crystal prior to entering the interferometer. The optical layout of the interferometer that combines the SH field with the PG field is shown in Fig. 1(a). The SH field is reflected by a dichroic beam splitter. The transmitted infrared (IR) pulses are converted to PG by a quartz plate and a quarter wave plate[4,5] then combined with the SH field. The chirped mirrors in the fundamental wave arm compensate the dispersion of the beam splitters and the birefringent optics.

There are two major drawbacks with the setup. The first one is high loss. For an input near-IR pulse energy of 750 μJ, the energy after the interferometer is 150 μJ, which is high enough for generating high harmonics with argon gas but not sufficient for neon and helium gases. The second drawback is the variation of the optical path length between the two arms due to vibration and thermal drift.

We developed a configuration to overcome those two drawbacks of the interferometer. Figure 1(b) shows the collinear setup for DOG, which is similar to what has been used for conventional PG except the quarter wave plate is now replaced by a quartz plate and BBO crystal. The laser pulses are sent to an initial quartz plate in order to generate two orthogonally polarized pulses with the required group delay between them that determines the PG width.[5] The optical axis of the quartz plate is oriented 45° with respect to the polarization direction of the input pulse. Its thickness of 410 μm generates a phase delay of 4.5 cycles between the ordinary wave and the extraordinary wave at center wavelength of 800 nm. The phase delay makes it an effective half-wave plate.

The two orthogonally polarized pulses are then sent to a second quartz plate with a thickness of 580 μm. Its optical axis is in the middle of the polarization of these two pulses. The beam then passes through a fused silica window with thickness of 0.5 mm into the vacuum chamber [not shown in Fig. 1(b)]. Finally, a BBO crystal with thickness of 150 μm generates the SH field. The optic axis of the BBO is aligned in the same plane as the second quartz plate. A large phase delay between the *o*-ray and *e*-ray of the IR beam was introduced by the second quartz plate. However, since the BBO crystal is negative uniaxial while the quartz is positive uniaxial, the two media compensate each other, thereby yielding a net phase delay of 5.75 cycles. Hence, the second quartz plate and the BBO combination forms a quarter wave plate for the IR pulses, which transforms the two linearly polarized pulses into two counter-rotating circularly polar-

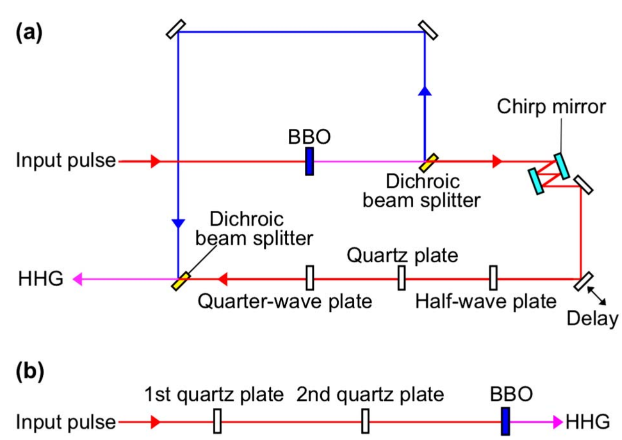

FIG. 1. (Color online) Experimental setups for double optical gating. (a) The SH field is added to the polarization gating field with a Mach–Zehnder interferometer. (b) The SH field and the gating field are generated and combined collinearly.

[a)]Electronic mail: chang@phys.ksu.edu.

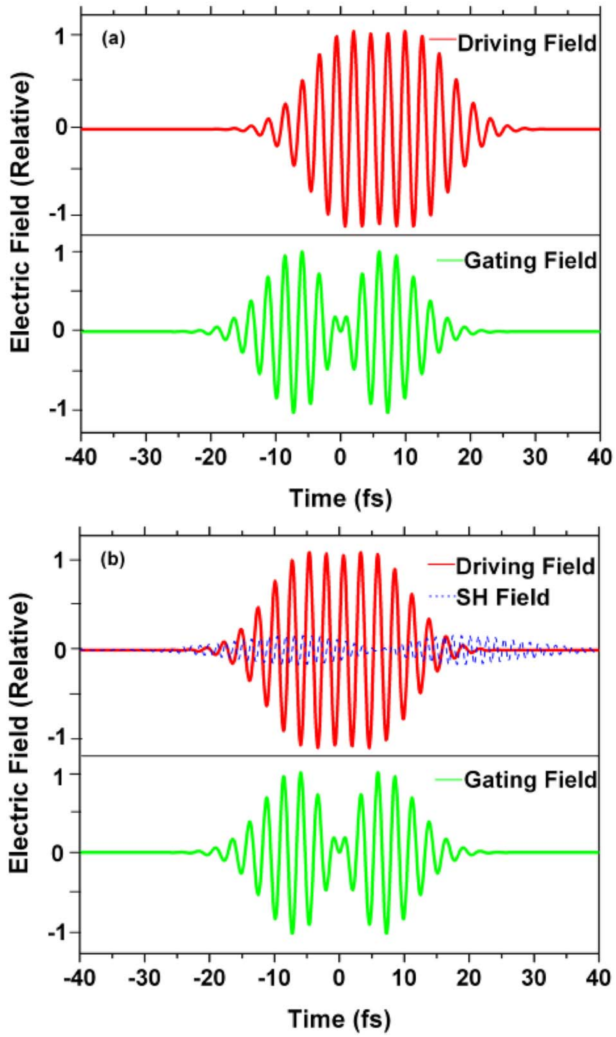

FIG. 2. (Color online) Laser fields in the collinear setup. (a) The driving and gating components after the second quartz plate. (b) The field components with the second harmonic (dashed line) contribution after the BBO crystal.

ized pulses for PG. This quartz plate was mounted in such a way that its face could be titled with respect to the beam propagation direction thereby allowing finer phase control over the phase difference between its own *o*-ray and *e*-ray. This is necessary for keeping the combination as a quarter wave plate when the BBO is tuned to optimize the SH generation.

The fundamental laser field after the BBO can be resolved into a driving field and orthogonally polarized gating field such as in the case of conventional PG, as shown in Fig. 2(a). The driving field is polarized in the same direction as the polarization direction of the SH field, which is required by the DOG. In other words, the SH field is generated from the gating field as the BBO is cut for type I phase matching. The group and phase velocities of the SH pulse and that of the fundamental driving field are different and as a result, the SH field from the first peak of the gating pulse overlaps with the fundamental driving field after the BBO, as shown in Fig. 2(b). The pulse duration of the SH is 20 fs as estimated using the software SNLO.[9] The setup thus combines the SH field to the polarization gating field for DOG without separating the two frequency components into two arms in space.

The highest energies of the fundamental and SH pulses achieved with the collinear setup are 750 and 75 μJ at the focus position, respectively. For comparison, the fundamental pulse from the interferometric setup is 150 μJ, thus, the throughput of the collinear setup is five times higher. When we set the optics for linear polarization, the pulse duration of the IR pulse was measured to be 9 fs using frequency resolved optical gating. The DOG beam was focused to the gas target with a mirror whose focal length is 400 mm. The intensities on the target could reach 1.4×10^{15} and 1.8×10^{14} W/cm^2 at the maximum energies. The higher intensity allowed us to generate high harmonics from neon gas, which was very difficult with the interferometric setup. The generated high harmonic spectrum was measured with an extreme ultraviolet (XUV) grating spectrometer.[10]

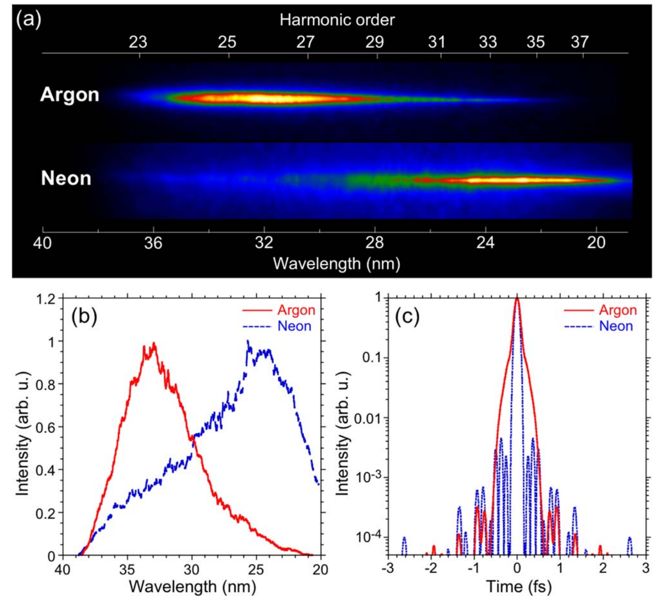

FIG. 3. (Color online) Comparison of argon and neon spectra generated. (a) The argon and neon supercontinuum images. (b) The line out plots of the normalized spectra for argon (solid line) and neon (dashed line). (c) The Fourier transforms of the spectra for argon (solid line) and neon (dashed line) from (b) assuming flat spectral phase.

Figure 3(a) shows typical harmonic spectra using argon and neon gases obtained with the collinear setup. The carrier-envelope (CE) phase of the IR pulses was stabilized during the data taking.[11] Unlike the interferometric setup, there is no relative phase jitter between the fundamental field and the SH field. The harmonic spectra have intensity distributions of supercontinuum, as shown in Fig. 3(b). The spectrum from neon gas shows a supercontinuum that covers a broad 20 nm plateau region. Figure 3(c) shows the Fourier transform limited pulses of argon and neon assuming a flat spectral phase. They are derived to be 180 and 130 as from those spectra, respectively. The results indicate that the temporal components do not contain the pre-/postpulse. The high input laser energy resulted in a high harmonic pulse energy of 0.14 nJ when argon was used as the target. This was measured with an XUV photodiode (model AXUV-100 from IRD, Inc.) and after a 0.2 μm aluminum filter used to eliminate the fundamental pulse.

For DOG, the high harmonic spectrum distribution as a function of the relative phase delay between the SH and the fundamental fields was measured by scanning the arm containing the fundamental beam of the Mach–Zehnder interferometer while the CE phase of the laser pulses was locked. The measured high harmonic spectra are shown in Fig. 4(a).

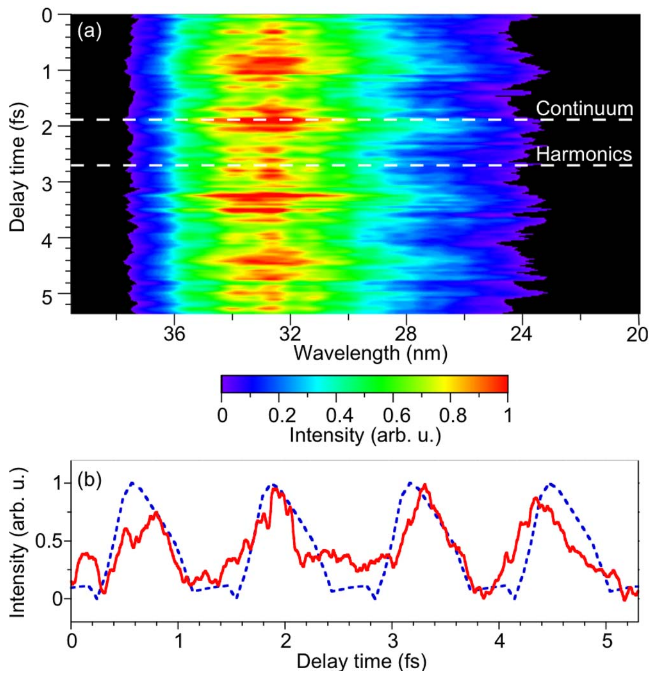

FIG. 4. (Color online) (a) The effects of a relative phase scan between the SH and fundamental pulses on the high harmonic spectrum. (b) Experimental (solid line) and calculated (dashed line) spectrally integrated signals.

The spectrally integrated signals show a half-cycle periodicity, as shown in Fig. 4(b). The high frequency fluctuations originated from the laser intensity variation were filtered out in the plotting. To produce single isolated pulses from every laser shot, the relative phase must be stabilized. However, the collinear method has no relative phase instabilities, which significantly simplified the construction and operation of the setup.

We studied CE phase effects with the collinear DOG. Figures 5(a) and 5(b) show high harmonic spectra as a function of CE phase sweep in the collinear and the interferometer DOG, respectively. The distribution in the collinear DOG is slightly different from the interferometer due to increased input intensity and optimized gas pressure. However, the periodicity of 2π is the same as in the case of the interferometer method.

In conclusion, we demonstrated a simpler and robust collinear setup for DOG, using only two quartz plates and a BBO crystal. As compared to the previously used interferometer setup, it has several advantages such as better relative phase stability between the fundamental and SH pulses, higher energy throughput, lower optics cost, and easier alignment. It allowed the generation of a supercontinuum supporting 130 as duration from neon gas using 9 fs long laser pulses. Also, with the correct choice of waveplate thickness, pulses as long as 12 fs can be used for collinear DOG.[6]

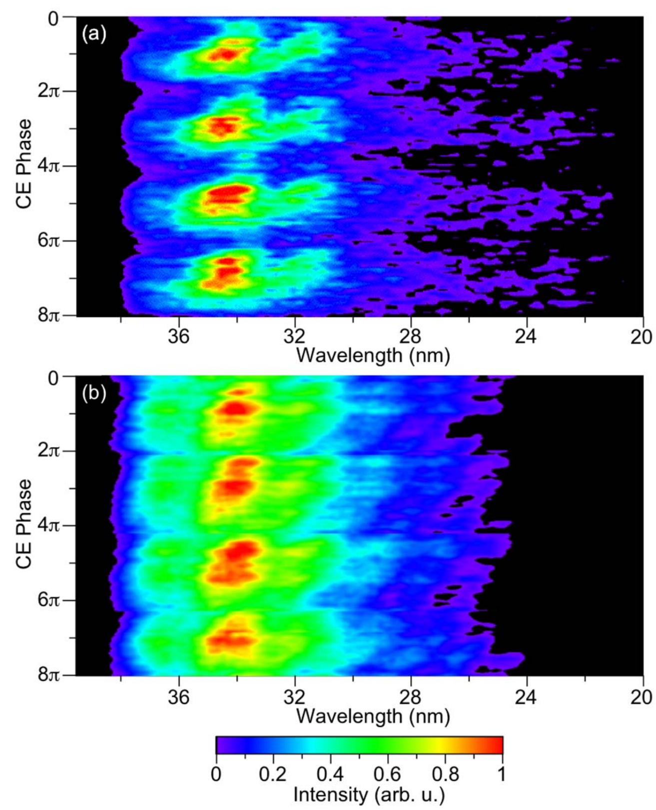

FIG. 5. (Color online) The effects of CE phase on the DOG high harmonic spectrum. The gating was applied with (a) the collinear method and (b) the interferometer method.

This material is supported by the NSF under Grant No. 0457269, by the U. S. Army Research Office under Grant No. W911NF-07-1-0475, and by the U.S. Department of Energy.

[1] G. Sansone, E. Benedetti, F. Calegari, C. Vozzi, L. Avaldi, R. Flammini, L. Poletto, P. Villoresi, C. Altucci, R. Velotta, S. Stagira, S. De Silvestri, and M. Nisoli, Science **314**, 443 (2006).
[2] P. Corkum, N. Burnett, and M. Ivnov, Opt. Lett. **19**, 1870 (1994).
[3] Z. Chang, Phys. Rev. A **70**, 043802 (2004).
[4] V. Platonenko and V. Strelkov, J. Opt. Soc. Am. B **16**, 030435 (1999).
[5] B. Shan, S. Ghimire, and Z. Chang, J. Mod. Opt. **52**, 277 (2005).
[6] H. Mashiko, S. Gilbertson, C. Li, M. S. Khan, M. Shakya, E. Moon, and Z. Chang, Attosecond Physics Workshop, Dresden, 1 August 2007 (unpublished).
[7] H. Mashiko, C. Nakamura, C. Li, E. Moon, H. Wang, J. Tackett, and Z. Chang, Appl. Phys. Lett. **90**, 161114 (2007).
[8] M. Nisoli, S. De Silvestri, O. Svelto, R. Szipcs, K. Ferencz, C. Spielmann, S. Sartania, and F. Krausz, Opt. Lett. **22**, 522 (1997).
[9] SNLO software website (http://www.sandia.gov/imrl/XWEB1128/snloftp.htm).
[10] M. Shakya, S. Gilbertson, H. Mashiko, C. Nakamura, C. Li, E. Moon, Z. Duan, J. Tackett, and Z. Chang, Proc. SPIE **6703**, 67030 (2007).
[11] C. Li, E. Moon, and Z. Chang, Opt. Lett. **31**, 3113 (2006).